Direct numerical simulation of a microramp in a high-Reynolds number supersonic turbulent boundary layer

Salvadore, Francesco; Memmolo, Antonio; Modesti, Davide; Della Posta, Giacomo; Bernardini, Matteo

DOI
10.1103/PhysRevFluids.8.110508

Publication date
2023

Document Version
Final published version

Published in
Physical Review Fluids

Gallery of Fluid Motion

Direct numerical simulation of a microramp in a high-Reynolds number supersonic turbulent boundary layer

Francesco Salvadore and Antonio Memmolo
HPC Department, CINECA, via dei Tizii 6/B, 00185 Rome, Italy

Davide Modesti
Aerodynamics group, Faculty of Aerospace Engineering, Delft University of Technology, Kluyverweg 2, 2629 HS Delft, The Netherlands

Giacomo Della Posta* and Matteo Bernardini
Department of Mechanical and Aerospace Engineering, Sapienza University of Rome, via Eudossiana 18, 00184 Rome, Italy

(Received 22 May 2023; published 16 November 2023)

This paper is associated with a video winner of a 2022 American Physical Society's Division of Fluid Dynamics (DFD) Gallery of Fluid Motion (GFM) Award for work presented at the DFD Gallery of Fluid Motion. The original video is available online at the Gallery of Fluid Motion, https://doi.org/10.1103/APS.DFD.2022.GFM.V0037

DOI: 10.1103/PhysRevFluids.8.110508

Shock wave/boundary layer interactions (SBLIs) can generate strong, intermittent thermomechanical loads and boundary layer separation [1], resulting in harmful consequences on the safety and performance of aerospace systems [2]. For this reason, several active and passive control solutions have been proposed to mitigate the negative effects of SBLI [3]. Microvortex generators (MVGs) are considered among the most promising passive control devices because they energize the boundary layer producing a system of trailing vortices, but they also induce limited wave drag because their height is lower than the boundary layer thickness. Possible applications of MVGs include for example the control of shock-induced separation occurring on transonic wings approaching buffet or in supersonic engine inlets.

The flow generated by a microramp in a supersonic turbulent boundary layer has been studied through experiments [4], Reynolds-averaged Navier-Stokes simulations (RANSs), and large-eddy simulations (LESs) [5–7], revealing the presence of primary and secondary vortices, as well as of almost-toroidal Kelvin-Helmholtz (KH) instabilities around the wake. Some studies have also performed parametric studies for different ramp geometries and free-stream Mach numbers and assessed the microramp performance [8,9], but a thorough characterization of the flow over a microramp using direct numerical simulation (DNS) is still missing, despite its potential to advance our understanding of these devices and to improve their control effectiveness.

*giacomo.dellaposta@uniroma1.it

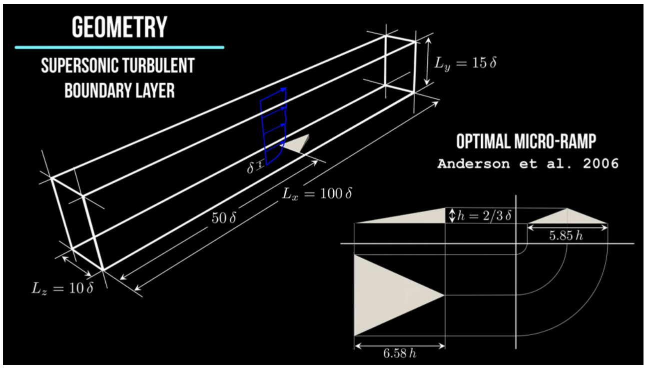

FIG. 1. Computational domain and geometry of the microramp.

In order to provide a careful description of this complex flow, in our recent work [10], we have quantified the effect of the Reynolds number on a supersonic boundary layer over a microramp developing a DNS data set at a remarkable friction Reynolds number.

The Gallery of Fluid Motion (GFM) video presents flow animations generated at runtime from these simulations, which used up to 1024 graphics processing units (GPUs) for 100-h runs collecting visualizations and statistics at the same time. We fix the free-stream Mach number $M_\infty = 2$ and consider three cases at friction Reynolds numbers $\mathrm{Re}_\tau = \rho_w u_\tau \delta/\mu_w = 500$, 1000, and 2000, where ρ_w and μ_w are the density and dynamic viscosity of the fluid at the wall, respectively, δ is the boundary layer thickness, $u_\tau = \sqrt{\tau_w/\rho_w}$ is the friction velocity, and τ_w the wall-shear stress.

Visualizations are rendered at runtime by coupling the *in situ* library Catalyst [11] from PARAVIEW [12] with our code supersonic turbulent accelerated Navier-Stokes solver (STREAmS) [13–15]. STREAmS is a high-order, finite-difference solver designed to tackle the compressible Navier-Stokes equations for a perfect, heat conducting gas in wall-bounded turbulent high-speed flows, and oriented to modern high-performance computing (HPC) platforms with multi-GPU architectures. *In situ* visualization dramatically limits the input/output (I/O) usage [16] thus making possible impressive flow visualizations of large-scale simulations with thousands of GPUs. The user can define the instants for flow visualizations and the variables sent to the Catalyst pipeline in the STREAmS input file. The pipeline is implemented by a PYTHON script which dynamically defines filters, camera, and graphical settings, finally producing the output images. The microramp geometry is based on the optimal shape defined by Anderson *et al.* [17] and is simulated using an immersed boundary method (IBM). A sketch of the geometry and of the computational domain is reported in Fig. 1. The finest, structured grid adopted for the high-Reynolds number simulation is made of approximately 30 billion mesh points—$16\,384 \times 896 \times 2048$ points in the streamwise, wall-normal, and spanwise directions, respectively. Instantaneous three-dimensional (3D) visualizations of the vortical structures [Fig. 2(a)] unravel the complex flow organization around the microramp, which include the formation of lateral counter-rotating vortices merging into the microramp wake, the so-called primary vortices, and the formation of a train of vortex rings that undergoes azimuthal instability and eventually breaks down in the wake. A comparison between flow cases at $\mathrm{Re}_\tau = 500$ and 2000 in Fig. 2(b) shows that increasing the Reynolds number enhances the coherence of the almost-toroidal vortical structures delimiting the wake, besides intensifying the turbulent activity in the boundary layer. Figure 3 shows the instantaneous streamwise velocity in wall-parallel planes at a distance $y^+ = y/\delta_v = 15$ and $y/\delta = 0.3$ from the wall, where $\delta_v = \mu_w/(\rho_w\, u_\tau)$ is the viscous length scale. Away from the wall [Fig. 3(b)], we clearly notice the footprint of the primary vortices at the ramp sides, which enhance momentum transfer bringing high-speed fluid close to the wall. In the near-wall region [Fig. 3(a)], we observe regions of high-speed flow induced by the large-scale transfer of momentum towards the wall, superposed to the typical small-scale streamwise

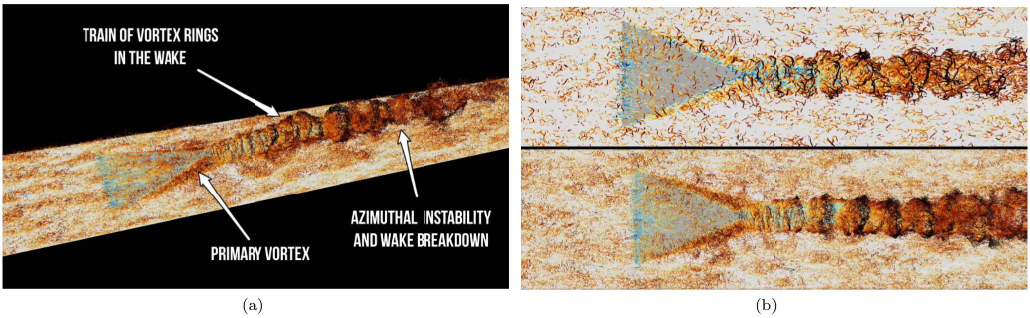

FIG. 2. Swirling strength isosurfaces coloured by streamwise velocity. (a) Main vortical structures at $\mathrm{Re}_\tau = 2000$. (b) Top view comparison of $\mathrm{Re}_\tau = 500$ (top) and 2000 (bottom).

streaks observed in canonical boundary layer flows [18]. The instantaneous density distribution on longitudinal [Fig. 4(a)] and cross-stream [Fig. 4(b)] planes shows that the shock structure is highly three dimensional and a complex shock system stems from the interaction of the supersonic flow with the microramp. A first shock originates from the leading edge of the ramp and soon becomes conical because of the three dimensionality of the microramp, whereas another conical shock is generated at the trailing edge. In addition, the trace of a KH instability in the shear layer is visible at the symmetry plane, where the vortex cores are recognizable in the top part of the wake, which gradually lifts up as a consequence of the upwash induced by the primary vortex pair. Vortex cores are not visible at the bottom of the wake, indicating that vortex rings do not completely close, differently from what previously supposed by Sun *et al.* [19].

Moreover, cross-stream planes also show the clear position of the two parallel primary vortices, whose azimuthal motion transfers high-momentum fluid close to the wall, energizing the boundary layer and thus enhancing its resistance to downstream separation.

In conclusion, our work demonstrates that *in situ* data processing allows us to obtain qualitative flow visualization for high-fidelity simulations at unprecedented computational scale. We believe that accurate flow visualization is a key tool at our disposal that should precede and complement the more canonical and quantitative data analysis. The level of detail and flow data accessibility provided by direct numerical simulation is in principle unparalleled, but extracting data from simulations of this size is challenging or even impossible when relying on a standard I/O method. In the present case, *in situ* visualizations have been essential to help us understand the wake overall qualitative structure, which previous studies had often only hypothesized. This was also helpful to guide the quantitative analysis and shed light on the flow physics of MVGs for the control of supersonic boundary layers.

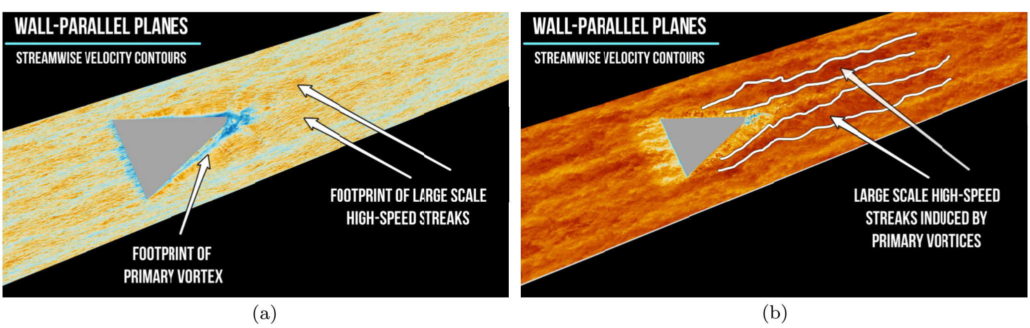

FIG. 3. Streamwise velocity contours on wall-parallel planes. (a) $y^+ = 15$. (b) $y/\delta = 0.3$.

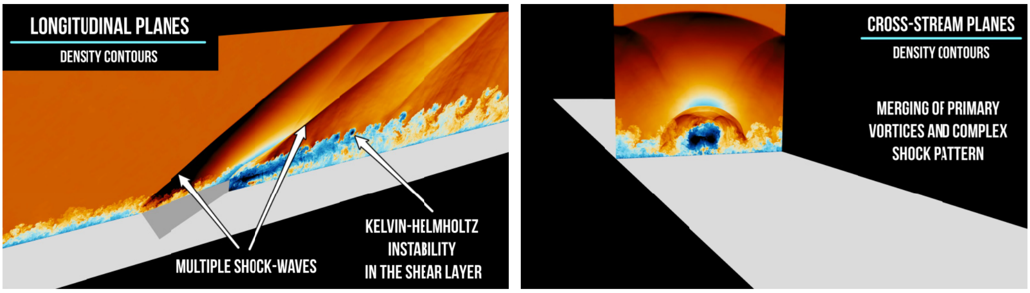

(a) (b)

FIG. 4. Density contours on (a) longitudinal and (b) cross-stream planes.

We acknowledge CINECA Casalecchio di Reno (Italy) for providing us with the computational resources required by this work.

[1] M. Bernardini, G. Della Posta, F. Salvadore, and E. Martelli, Unsteadiness characterisation of shock wave/turbulent boundary-layer interaction at moderate Reynolds number, J. Fluid Mech. **954**, A43 (2023).
[2] D. V. Gaitonde, Progress in shock wave/boundary layer interactions, Prog. Aerosp. Sci. **72**, 80 (2015).
[3] H. Babinsky and H. Ogawa, SBLI control for wings and inlets, Shock Waves **18**, 89 (2008).
[4] N. Titchener and H. Babinsky, A review of the use of vortex generators for mitigating shock-induced separation, Shock Waves **25**, 473 (2015).
[5] F. K. Lu, Q. Li, and C. Liu, Microvortex generators in high-speed flow, Prog. Aerosp. Sci. **53**, 30 (2012).
[6] Z. Sun, F. Scarano, B. W. van Oudheusden, F. F. J. Schrijer, Y. Yan, and C. Liu, Numerical and experimental investigations of the supersonic microramp wake, AIAA J. **52**, 1518 (2014).
[7] A. G. Panaras and F. K. Lu, Micro-vortex generators for shock wave/boundary layer interactions, Prog. Aerosp. Sci. **74**, 16 (2015).
[8] R. H. M. Giepman, A. Srivastava, F. F. J. Schrijer, and B. W. van Oudheusden, Mach and Reynolds number effects on the wake properties of microramps, AIAA J. **54**, 3481 (2016).
[9] S. Tambe, F. F. J. Schrijer, and B. W. van Oudheusden, Relation between geometry and wake characteristics of a supersonic microramp, AIAA J. **59**, 4501 (2021).
[10] G. Della Posta, M. Blandino, D. Modesti, F. Salvadore, and M. Bernardini, Direct numerical simulation of supersonic boundary layers over a microramp: Effect of the Reynolds number, J. Fluid Mech., doi:10.1017/jfm.2023.764.
[11] A. C. Bauer, B. Geveci, and W. Schroeder, *The ParaView Catalyst User's Guide v1.0* (Kitware, 2013).
[12] J. Ahrens, B. Geveci, and C. Law, ParaView: An end-user tool for large data visualization, in *Visualization Handbook* (Elsevier, Amsterdam, 2005).
[13] M. Bernardini, D. Modesti, F. Salvadore, and S. Pirozzoli, STREAmS: A high-fidelity accelerated solver for direct numerical simulation of compressible turbulent flows, Comput. Phys. Commun. **263**, 107906 (2021).
[14] M. Bernardini, D. Modesti, F. Salvadore, S. Sathyanarayana, G. Della Posta, and S. Pirozzoli, STREAmS-2.0: Supersonic turbulent accelerated Navier-Stokes solver version 2.0, Comput. Phys. Commun. **285**, 108644 (2023), https://github.com/STREAmS-CFD/STREAmS-2.
[15] S. Sathyanarayana, M. Bernardini, D. Modesti, S. Pirozzoli, and F. Salvadore, High-speed turbulent flows towards the exascale: STREAmS-2 porting and performance, arXiv:2304.05494.
[16] S. Klasky, H. Abbasi, J. S. Logan, M. Parashar, K. Schwan, A. Shoshani, M. Wolf, S. Ahern, I. Altintas, W. Bethel, L. Chacón, C. Chang, J. H. Chen, H. Childs, J. C. Cummings, S. Ethier, R. W. Grout, Z. Lin,

Q. Liu, X. Ma *et al.*, *In situ* data processing for extreme-scale computing, in *Proceedings of the SciDAC* (Academia Press, London, 2011), pp. 1–16.
[17] B. Anderson, J. Tinapple, and L. Surber, Optimal control of shock wave turbulent boundary layer interactions using micro-array actuation, in *Proceedings of the 3rd AIAA Flow Control Conference* (AIAA, Reston, VA, 2006).
[18] S. J. Kline, W. C. Reynolds, F. A. Schraub, and P. W. Runstadler, The structure of turbulent boundary layers, J. Fluid Mech. **30**, 741 (1967).
[19] Z. Sun, F. F. J. Schrijer, F. Scarano, and B. W. van Oudheusden, The three-dimensional flow organization past a micro-ramp in a supersonic boundary layer, Phys. Fluids **24**, 055105 (2012).